Automatic detection and tracking of coronal bright points in SDO/AIA images

I. Dorotovič [1,2], A. Coelho [2], J. Rybák [3], A. Mora [2], R. Ribeiro [2], W. Kusa [4], R. Pires [2]

[1] Slovak Central Observatory, Hurbanovo, Slovak Republic
[2] CTS/UNINOVA-CA3, FCT-UNL, Caparica, Portugal
[3] Astronomical Institute SAS, Tatranská Lomnica, Slovak Republic
[4] Faculty of Physics and Applied Computer Science, AGH University of Science and Technology, Kraków, Poland

E mail (ivan.dorotovic@suh.sk).

Abstract The AIA instrument, on-board the SDO satellite, provides high-resolution and high-cadence solar images since 2010. To extract scientific knowledge about coronal bright points (CBPs) from those high-resolution images there is a need for efficient automatic algorithms to detect and/or track the CBPs. In the last decade other research teams have developed algorithms to obtain more precise estimations of the solar rotation profile. However, it is a difficult task because CBPs may change shape and size over time, yielding great difficulty to track them.
In this work we discuss the usage of two automatic segmentation algorithms to detect CBPs in SDO/AIA images: (1) using SunPy and OpenCV in Python and (2) using a Gradient Path Labeling (GPL) algorithm. Our preliminary tests and results, with a three-day dataset, show that these algorithms are promising tools to help refine the solar rotational profile.

Introduction

Coronal bright points (CBPs) are small and bright structures observed in the extreme ultraviolet (EUV) part of the solar spectrum. While sunspots are concentrated in two bands, migrating from mid-latitudes to the equator, CBPs can be found all over the Sun, even appearing at the poles and in coronal holes. This unique feature allows researchers, after detecting and tracking them over a sequence of images, to understand the Sun's rotational speed, which is known to be differential. Since 2010 the AIA instrument (Lemen et al., 2012), on-board the SDO satellite (Pesnell et al., 2012), provides high-resolution and high-cadence solar images. Hence, we have now access to huge amounts of high-resolution solar images, which require efficient automatic image processing tools to detect and/or track solar activity features. In the last decade, research teams have already developed algorithms to obtain more precise estimations of the solar rotation profile (e.g. Zharkova 2005, McIntosh and Gurman 2005, Martens 2012, Sudar et al. 2016, among others).

Shahamatnia et al. (2016a) first applied a PSO/Snake hybrid algorithm for tracking CBPs and calculating solar differential rotation. Second, Shahamatnia et al. (2016b) compared the PSO/Snake hybrid algorithm with the Gradient Path Labeling (GPL) segmentation algorithm (proposed by Mora et al. 2011), using benchmark SDO/AIA images. In this paper we extended the latter work by combining both the segmentation algorithm developed using SunPy and OpenCV in Python (Hughitt, 2012, Bradski, 2000) and the GPL (Gradient Path Labeling) segmentation algorithm (Mora et al. 2011), associated with a region matching process to identify and track the CBPs.

Case Study Data

Our case study includes SDO/AIA FITS images from the 13.1 nm and 19.3 nm wavelengths, with 4096x4096 pixels, for the period 9 – 11 August 2010, constituting a total of 430 images from the three-day sample. The cadence of images is 10 minutes and the resolution is 0.6″. The fully photometrically reduced SDO/AIA images are used in this work (SolarSoft: aia_prep.pro) after removing the SDO/AIA point-spread-function effect (Poduval et al., 2013).

Algorithm 1: SunPy and OpenCV in Python

We used a segmentation algorithm using SunPy and OpenCV in Python (Hughitt, 2012, Bradski, 2000) for automatic detection of CBPs. The algorithm is illustrated in Figure 1 with the case study dataset. First step of the algorithm is the extraction of corona from the SDO/AIA images, using information stored in the FITS files, or by fitting a circle using a Hough transform. Solar images are then converted and down sampled to the resolution of 1024x1024. Gaussian blur with kernel size 7x7 and both σ_x, σ_y are calculated using kernel size to remove noise from the image. Next step is to apply the CLAHE (Contrast Limited Adaptive Histogram Equalization) algorithm (Pizer et al., 1987) with window size 8x8, corresponding to the average size of CBPs (Figure 1 b). Adaptive thresholding is then used for binarization of the image (Figure 1 c). After, morphological operators (erosion, closing and opening) are applied to enhance features of CBPs (Figure 1 d).

At this stage the image is ready to be labelled using Blob Detector from OpenCV library. Blobs are defined as circular shapes with maximum area of 80 pixels and their center of mass is calculated. Finally, detected CBPs are filtered to exclude the brightest active regions and their neighbourhoods. Images from different wavelengths were used to test the algorithm. The results with 19.3nm wavelength (Figure 1 e)) are more accurate for the lower solar latitudes. On the other side, the 13.1nm wavelength (Figure 1 f)) proved to be more accurate for the polar coronal holes. Additional tests were performed with 9.4 nm wavelengths but the results were less satisfactory.

Algorithm 2: Gradient Path Labeling (GPL)

The GPL segmentation algorithm was initially designed and proposed by Mora et al. (2011) to segment retinal images. Shahamatnia et al. (2016b) confirmed that the segmentation and tracking of CBPs in solar images is also a promising domain for the application of GPL, since CBPs are higher intensity regions with distinguishable boundaries. SDO/AIA images have been chosen to test and adjust the GPL algorithm capabilities. Due to GPL algorithm complexity being proportional to the high resolution of images, the original images were divided into 16 smaller regions and the segmentation and CBPs detection was

applied separately to each one. The GPL approach to segment CBPs follows a three step process that starts by pre-processing the image to reduce noise, followed by its segmentation. Finally, the generated segmentation regions are filtered to select the region that matches any CBP, and their center of mass location is also determined. Figures 2 illustrates the segmentation and remerge process of the GPL algorithm. More details on the image pre-processing, the GPL segmentation and CBP matching can be found in Coelho (2017) and Dorotovič et al. (2017).
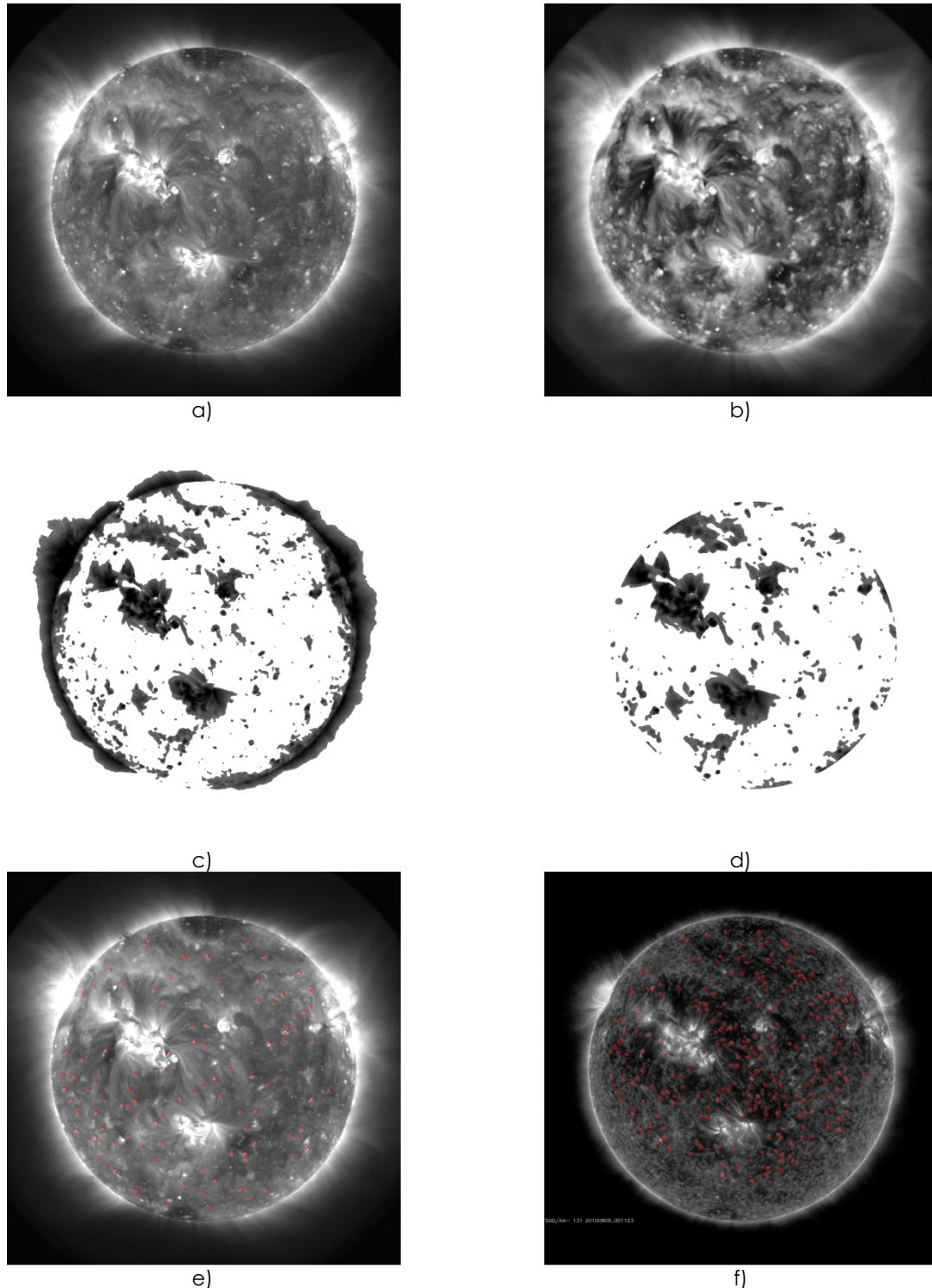
Figure 1. Illustrative images of the CBPs detection process: a) original solar image in the 19.3 nm channel with Gaussian blur, b) after application of CLAHE (Contrast Limited Adaptive Histogram Equalization), c) after thresholding, d) after morphological operators, e) final results of the CBPs detection in 19.3nm channel, f) final results for the 13.1 nm channel for comparison.
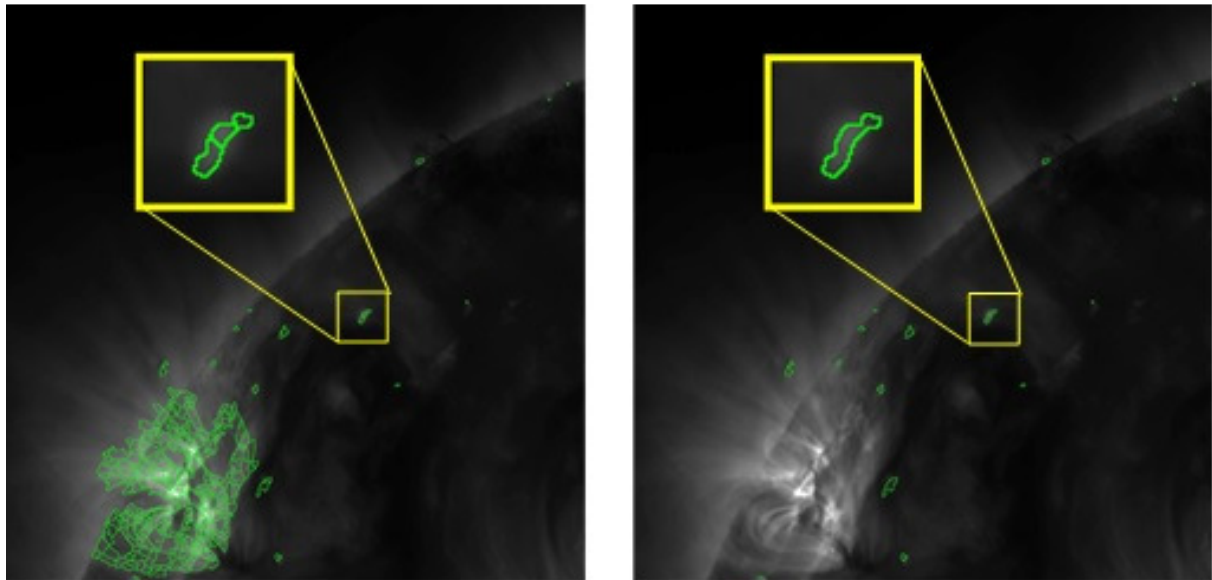
Figure 2. Top panel: Remerge illustration with a highlighted region: result of GPL segmentation (left) and after remerge operation (right). The contour of the GPL segmented objects is displayed in green. Source: Dorotovič et al. (2017)
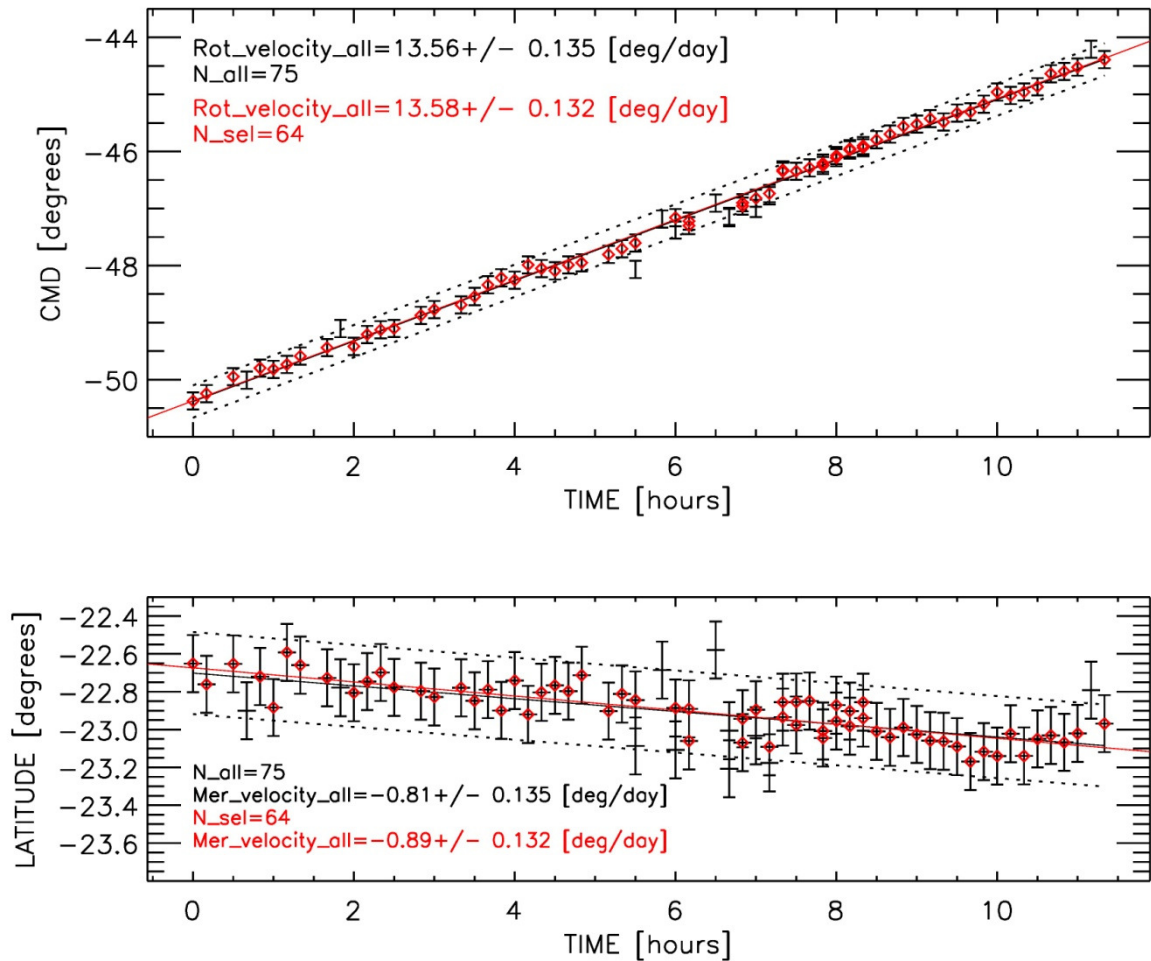

Figure 3. Temporal evolution of the identified longitude (upper graphic) and latitude (lower graphic) positions of a longer-lived CBP. The error bars display all observed coordinates and estimation of their uncertainty of the CBP. The solid and dotted lines show a linear fit and the 1-σ error of the fit, respectively. *Source: Dorotovič et al. (2017).*
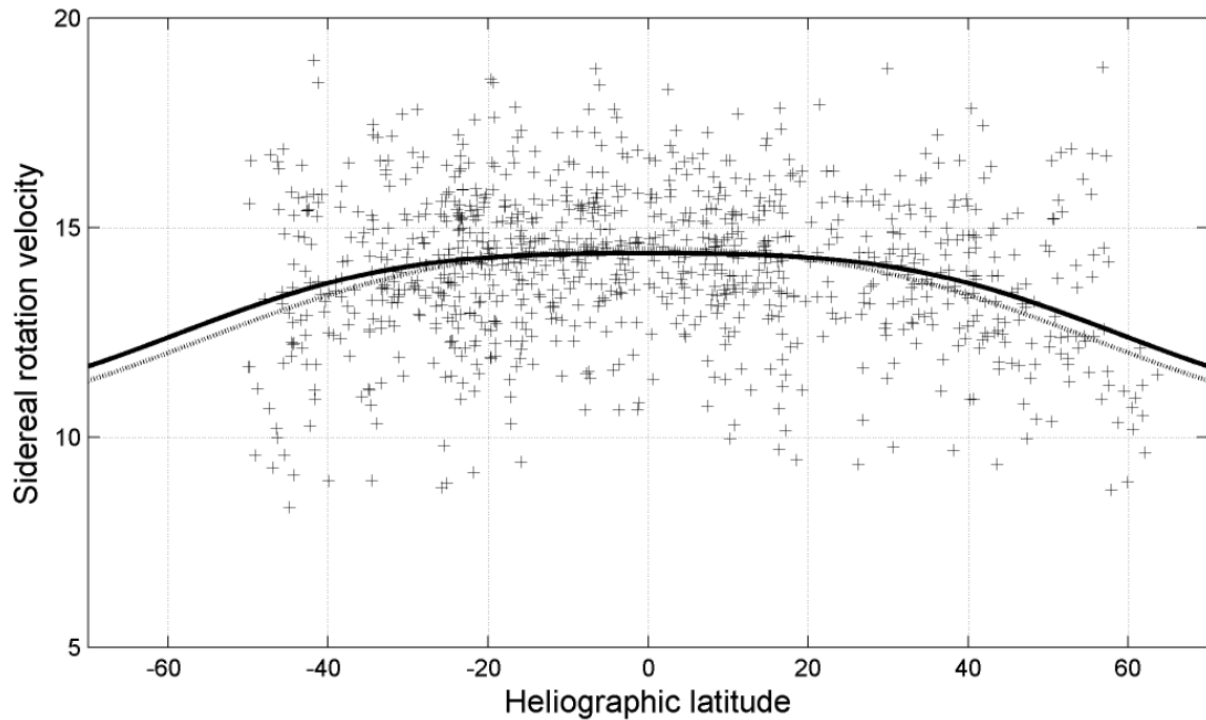
Figure 4. Individual observations of rotational velocity in respect to latitude. Thick solid black line indicates the best fit to these values. The values of the optimum fit (solid line) parameters A, B, C are 14.392 ° day^{-1}, −0.567 ° day^{-1}, and −2.8 ° day^{-1}, respectively.

With the case study full dataset (3 days) GPL detected a total of 75881 CBPs inside 85% of the solar radius in 430 images. It means on average 176 CBPs per image. After tracking, only the CBPs that contained 15 or more observations were selected, obtaining a total of 557 CBPs. For comparison, Sudar et al. (2015) identified during 2 studied days a total of 906 CBPs with 10 consecutive identifications (observations). In addition, following Sudar approach we also computed the sideral rotation velocity (ω_{rot}) and meridional velocity (ω_{mer}) and filtered to $8° < \omega_{rot} < 19°$ day^{-1} and $-4° < \omega_{mer} < 4°$ day^{-1} to remove outliers.

To illustrate the GPL tracking capability for a particular longer-lived CBP, Figure 3 displays the temporal evolution with longitude and latitude coordinates. Numerical results for both the rotational and meridional velocities derived from all coordinates are also given in the Figure.

Solar Rotational Profile

Figure 4 shows the solar differential rotational profile obtained with the GPL three days results. The solid line depicts the fitting relation used: $\omega = A + B.sin^2 b + C.sin^4 b$. The coefficients obtained, which best fit the dependence of the angular velocity ω on the heliographic latitude b, are as follows: A = 14.392 ± 0.0159 ° day^{-1}, B = −0.567 ± 0.157 ° day^{-1}, and C = −2.8 ± 0.138 ° day^{-1}.

Conclusions

We tested two algorithms that automatically detect and track CBPs in 19.3 nm and 13.1 nm solar images from the SDO/AIA instrument at 10 min cadence. The results obtained confirmed that the algorithms constitute promising tools for processing massive solar image archives as well as to investigate the evolution of solar activity and space weather effects. Both algorithms have the ability to detect CBPs on different wavelengths with some parameters tuning. This is an advantage over other approaches since it's possible to merge the results from different wavelengths to get a more accurate CBPs detection on the entire solar corona, including high latitudes and polar coronal holes located CBPs. However, the size of the scatter in Figure 4 is quite great and this suggests that the tracking method needs further improvement.

References

Bradski, G.: 2000, The OpenCV Library. Dr. Dobb's Journal of Software Tools.

Coelho, A.: 2017, Solar rotation speed by detecting and tracking of Coronal Bright Points, MSc Thesis, FCT-UNL, Lisbon (Portugal).

Dorotovič, I., Coelho, A., Rybák, J., Mora, A., Ribeiro, R.: 2017, Gradient Path Labelling method and tracking method for calculation of solar differential rotation using coronal bright points, Astronomy and Computing, submitted.

Hughitt, K., Christe, S., Mayer, F., Earnshaw, M., Mumford, S., Ireland, J., Shih, A., Perez-Suarez, D. et al.: 2012, SunPy: Open Source Solar Data Analysis Tools for Python.

Lemen, J. R., Title, A. M., Akin, D. J., et al. 2012, The Atmospheric Imaging Assembly (AIA) on the Solar Dynamics Observatory (SDO), Sol. Phys., 275, 17

Martens, P.: 2012, Image Recognition and Feature Detection in Solar Physics, AAS Meeting #220, id.323.02.

McIntosh, S. W., Gurman, J. B.: 2005, Nine Years Of Euv Bright Points. Solar Physics 228, 285.

Mora, A.D., Vieira, P.M., Manivannan, A., Fonseca, J.M.: 2011, Automated drusen detection in retinal images using analytical modelling algorithms. Biomed. Eng. Online. 10, 59.

Pizer, S. M., Amburn, E. P., Austin, J. D. et al.: 1987, Adaptive Histogram Equalization and Its Variations. Computer Vision, Graphics, and Image Processing 39, 355.

Poduval, B., DeForest, C. E., Schmelz, J. T. and Pathak, S.: 2013, Point-spread Functions for the Extreme-ultraviolet Channels of SDO/AIA Telescopes, The Astrophysical Journal, 765, 144.

Pesnell, W. D., Thompson, B. J., Chamberlin, P. C., Jan. 2012. The Solar

Dynamics Observatory (SDO). Solar Physics 275, 3.

Shahamatnia, E., Dorotovič, I., Fonseca, J.M., Ribeiro, R.A.: 2016a, An evolutionary computation based algorithm for calculating solar differential rotation by automatic tracking of coronal bright points. J. Sp. Weather Sp. Clim. 6, A16.

Shahamatnia, E., Mora, A., Dorotovič, I., Ribeiro, R.A., Fonseca, J.M.: 2016b, Evaluative Study of PSO/Snake Hybrid Algorithm and Gradient Path Labeling for Calculating Solar Differential Rotation, Trans. on Comput. Coll. Intelligence XXIV, 19.

Sudar, D.; Skokić, I.; Brajša, R.; Saar, S. H.: 2015, Steps towards a high precision solar rotation profile: Results from SDO/AIA coronal bright point data, Astron. and Astrophys., 575, A63.

Sudar, D., Saar, S. H., Skokić, I., Poljančić Beljan, I., Brajša, R.: 2016, Meridional motions and Reynolds stress from SDO/AIA coronal bright points data, Astronomy and Astrophysics, 587, A29.

Zharkova, V. V., Aboudarham, J., Zharkov, S., Ipson, S. S., Benkhalil, A. K., Fuller, N.: 2005, Solar Feature Catalogues in Egso, Solar Phys., 228, 361.